metals

MDPI

Article

The Influence of Assembly Force on the Material Loss at the Metallic Head-Neck Junction of Hip Implants Subjected to Cyclic Fretting Wear

Khosro Fallahnezhad [1], Reza H. Oskouei [1,*], Hojjat Badnava [2] and Mark Taylor [1]

[1] College of Science and Engineering, Flinders University, Clovelly Park, SA 5042, Australia; khosro.fallahnezhad@flinders.edu.au (K.F.); mark.taylor@flinders.edu.au (M.T.)
[2] Discipline of Mechanical Engineering, Behbahan University of Technology, Behbahan 6361647189, Iran; ha.badnava@me.iut.ac.ir
* Correspondence: reza.oskouei@flinders.edu.au; Tel.: +61-8-8201-2782

Received: 2 March 2019; Accepted: 3 April 2019; Published: 8 April 2019

check for updates

Abstract: The impaction force required to assemble the head and stem components of hip implants is proven to play a major role in the mechanics of the taper junction. However, it is not clear if the assembly force could have an effect on fretting wear, which normally occurs at the junction. In this study, an adaptive finite element model was developed for a CoCr/CoCr head-neck junction with an angular mismatch of 0.01° in order to simulate the fretting wear process and predict the material loss under various assembly forces and over a high number of gait cycles. The junction was assembled with 2, 3, 4, and 5 kN and then subjected to 1,025,000 cycles of normal walking gait loading. The findings showed that material removal due to fretting wear increased when raising the assembly force. High assembly forces induced greater contact pressures over larger contact regions at the interface, which, in turn, resulted in more material loss and wear damage to the surface when compared to lower assembly forces. Although a high assembly force (greater than 4 kN) can further improve the initial strength and stability of the taper junction, it appears that it also increases the degree of fretting wear. Further studies are needed to investigate the assembly force in the other taper designs, angular mismatches, and material combinations.

Keywords: fretting wear; CoCrMo alloys; assembly force; material loss; modular hip implants; finite element

1. Introduction

Modular junctions are commonly used in orthopaedics, such as the head-neck taper junction in total hip replacement, to allow flexibility at the time of surgery. The aim is to generate a rigid connection between the modular components. However, fretting wear occurs due to the small-amplitude relative motions that occur at the interface under physiological loads in the body. In addition, fretting wear can remove the passive oxide layer of the metal alloy, and, with the presence of the body fluid, re-passivation occurs within the small crevice at the junction, which causes fretting corrosion [1,2]. These phenomena produce particulate debris and metal ions, which, in turn, can cause adverse local tissue reactions and, ultimately, clinical failure [3–5].

The mechanical behavior of the taper connection is dependent on a number of parameters. The material combination used at the taper [6] and the taper mismatch angle [6–9] can be controlled by the design and the manufacturing process. The type of the mechanical load as a result of daily activities can also influence the mechanical behavior of the taper junction [10,11]. Since the components are assembled intraoperatively, the assembly force is important not only to avoid loosening and dissociation after implantation [12,13] but also to establish a favorable mechanical environment to minimize fretting. There is variation between the manufacturers' recommendations on how to impact the femoral head [14], from a single light tap to several sharp hammer blows. The impaction forces generated by surgeons can vary significantly from approximately 300 N to an excess of 7500 N [15]. To date, the majority of studies [12,16–18] investigating the influence of the assembly force have focused on the dissociation force as the metric to assess the performance of the taper. Assembly forces from 2 kN to 15 kN have been investigated and a linear relationship with the dissociation force has been reported [12,16]. The dissociation force is always lower and varies between 42% [17] and 91% [18] of the assembly force. Rehmer et al. [12] reported a similar linear relationship between the assembly force and the twist off torque. Increasing the impaction force has also been shown to increase the contact area [6,19] and reduce the micro-motion [18,20] between the head and the trunnion. These studies generally suggest that a high assembly force can achieve a high degree of initial stability and fixation in the head-neck junction to more reliably withstand mechanical loads of daily activities without disconnection.

However, very few studies have attempted to address the important question of whether the assembly force has an influence on the material removal by fretting wear over an extended period. Bitter et al. [18] developed a combined experimental and finite element (FE) study to analyze the influence of assembly force (2, 4, and 15 kN) on the fretting wear of a Ti-6Al-4V femoral stem in contact with a Ti-6Al-4V taper adaptor. Their experimental results showed large standard deviations in terms of volumetric wear and no significant difference was found between the three tested assembly forces. However, it was reported that, when increasing the assembly force, the fretting wear reduces at the taper interface. They also used a simplified FE modelling approach simulating accelerated fretting (did not incorporate geometry updates to account for material loss). Employing a simplified version of the Archard equation, they defined a total wear score for the interface using the contact pressure and relative micro-motion for each contact node. As a major simplification, their model was not able to track the fretting wear process over several cycles of sliding. No correlation was found between the predicted wear scores (from the FE analysis) and the experimental volumetric wear [18]. In another FE analysis, English et al. [21] modelled a CoCr head and a titanium neck with a zero angular mismatch to estimate the material loss and contact pressure at the junction subjected to two million cycles of walking gait loading. This work was extended to explore the influence of assembly force, and they reported that higher assembly forces resulted in lower fretting wear [22]. However, they still used the critical simplification of zero angular mismatch for the junction in the dry condition. The materials modelled in the previous studies did not include the common combination of CoCr head and CoCr neck. Furthermore, the existing taper angle mismatch between the head and neck components has been ignored in the previous fretting wear studies while the angular mismatch has been found to significantly influence the mechanics of the junction [6,23]. Therefore, it could have a significant effect on fretting wear as a mechanically driven process. More importantly, the previous FE simulations have often assumed a dry condition for the contacting materials of the junction. However, the existence of body fluid at the interface of the junction may control the frictional characteristics and wear characteristics, which may influence the fretting wear behavior.

This work aims to simulate the fretting wear process and predict the material removal in a CoCr/CoCr head-neck junction through an adaptive finite element modelling approach. To achieve more realistic outcomes, the taper junction was modelled to have a distal contact with a real angular mismatch between the head and neck with the presence of simulated physiological body fluid. The main research objective was to evaluate the effect of assembly force on the material loss and fretting wear process in this type of taper junction.

2. Methods

A 3D model of a 32-mm diameter CoCr head with a 12/14 CoCr neck (as per dimensions reported by Rehmer et al. [12]) was first analyzed under normal walking load profiles [24,25] in order to determine the most critical plane of the taper junction in terms of two important fretting wear parameters of normal contact stress (contact pressure) and micro-motion. An elastic-plastic material model was used for CoCr (ISO 5832-12) with a Young's modulus of 210 GPa, Poisson's ratio of 0.30, yield stress of 910 GPa, ultimate tensile stress of 1350 GPa, and tensile elongation of 15%. The contact pressure and displacement were retrieved for all the nodes in the contacting regions of the head and neck, using a Python script, under the maximum force and moment of the loading profile. The relative displacements (micro-motions) of the contacting nodes were then determined using a MATLAB code. The middle plane passing through the superolateral region of the neck was found as the most critical plane to have the largest area of contact pressure (as shown in Figure 1) together with micro-motions. This critical plane was then employed for the main 2D fretting wear model that will be described next.

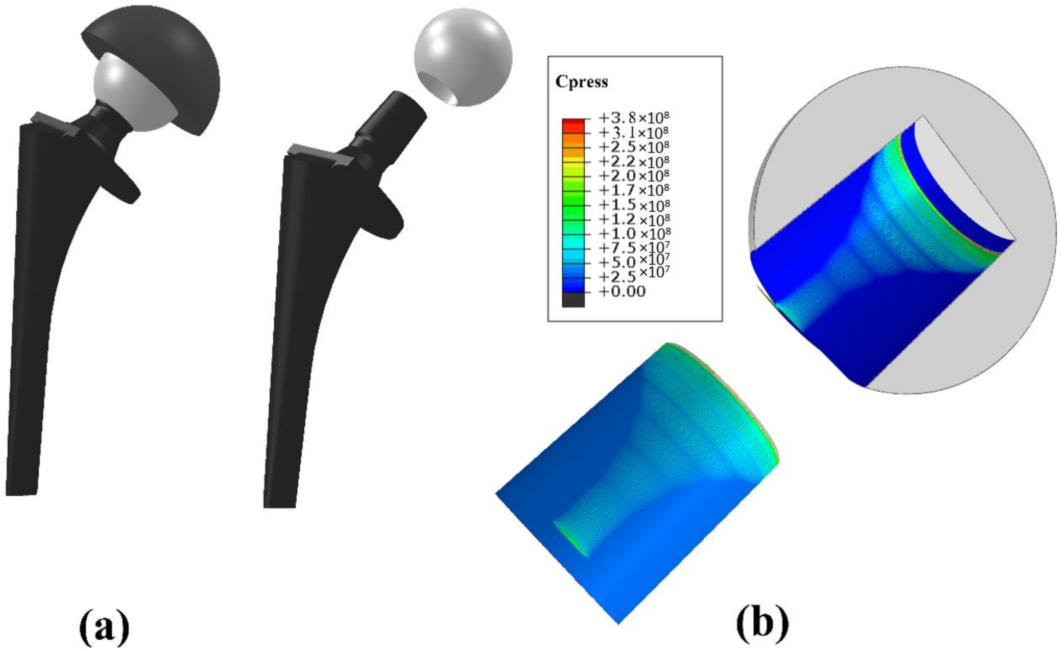

Figure 1. (**a**) A three-dimensional model of a hip joint implant and (**b**) distribution of contact pressure (in Pa) in both the head and neck under a normal walking gait loading, which indicates that the super-lateral region has the largest contacting area with both contact pressures and micro-motions.

2.1. Fretting Wear Model Development

The Archard wear formulation (Equation (1)) [26] was used in the fretting wear model of this work:

$$\frac{V}{S} = k\frac{F}{H} \tag{1}$$

where V (m^3) is the lost volume, S (m) is the amplitude of sliding, k (Pa^{-1}) is the wear coefficient, F (N) is the normal force, and H is the hardness of the material [26]. The Archard formulation can be localized and applied to the points of a contact region, which makes it suitable for FE simulations. In addition, the Archard equation has been previously used for fretting wear simulations with success [27–30].

Dividing both sides of the Archard wear equation (Equation (1)) by the area, yields the following.

$$h = K{\cdot}S{\cdot}p{\cdot}\Delta N \tag{2}$$

where h (m) is the depth of wear, K is the wear coefficient-to-hardness ratio (k/H), p (Pa) is the normal contact stress, and ΔN is the load cycle update interval. The main reason to re-write Equation (1) in the form of Equation (2) was to apply the Archard formula to the contacting nodes in the FE model. For the fretting wear model in the present study, a FORTRAN code was developed to trace and determine the positioning of the contacting nodes through the ABAQUS UMESHMOTION subroutine within an adaptive meshing constraint.

2.1.1. Verification

McColl et al. [29] and Ding et al. [28] developed an algorithm based on the Archard equation in order to simulate fretting wear for a pin-on-disc testing system. They reported surface profiles of the disc after various cycles of fretting wear. In order to verify the UMESHMOTION code developed for the head-neck junction in this study, a pin-on-disc model was first generated to replicate the Ding's model. This model had a very similar configuration (materials, geometry, element sizes, meshing structure, normal force, and sliding amplitude and frequency). The surface of the disc after the fretting wear process was evaluated (Figure 2) and compared with the results reported by Ding et al. [28]. Table 1 provides a comparison between the results of this study and those presented by Ding et al. [28] in terms of the width and height of the wear profile for the disc, which shows a very good level of agreement and verifies the UMESHMOTION code and its accuracy used in this study.

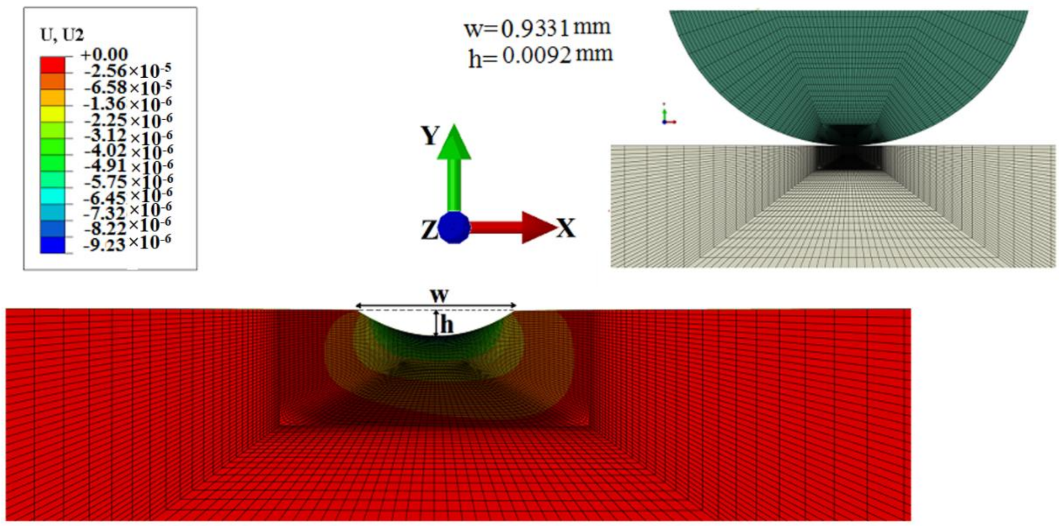

Figure 2. The distribution of displacement in the Y-axis (in meters) representing material removal from the surface of the disc under a normal force of 1200 N and a sliding amplitude of 10 µm after 18,000 cycles of fretting wear.

Table 1. The width and height of the wear profile for the disc after various fretting wear test cycles. A comparison between the computational results of this work and those presented by Ding et al. [28].

Comparison	Wear Profile Parameters on the Surface of the Disc	After 1000 Cycles	After 5000 Cycles	After 18,000 Cycles
Results of this work	Width, w (mm)	0.3512	0.7123	0.9331
	Height, h (mm)	0.0013	0.0042	0.0092
Results reported by	Width, w (mm)	0.3834	0.7644	0.9754
	Height, h (mm)	0.0013	0.0042	0.0092

2.1.2. Fretting Wear Model for the Head-Neck Taper Junction

The most critical plane of the head-neck junction that was previously identified by the 3D FE analysis was used to develop a 2D fretting wear model for the taper junction. Figure 2 illustrates the mesh structure of the 2D head-neck junction model and the profile of the corresponding force components (from the normal walking gait cycle) applied to this plane.

For the Archard wear equation (Equation (2)), the wear coefficient-to-hardness ratio (K) for the CoCr/CoCr head-neck combination was determined from a set of experimental results reported by Maruyama et al. [31]. They employed CoCr/CoCr pin-on-disc experiments under various normal contact stresses and sliding cycles in a phosphate buffered saline (PBS) condition. From their results and using the Archard equation, the wear coefficient-to-hardness ratio was determined for nine cases tested in their study. The nine K values were found to be very close with a maximum difference of 10% from which an average of $K = 1.7 \times 10^{-15}$ Pa^{-1} was calculated and used for the CoCr/CoCr taper junction model.

The coefficient of friction between CoCr and CoCr in the PBS condition was also obtained from the results reported by Maruyama et al. [31]. Their results for different contact stresses and cycles showed that the friction coefficient becomes constant at 0.60 after approximately 5000 cycles, which was used in the FE simulations of this work.

The authors' previous work [23] showed that head-neck taper junctions with distal angular mismatches have generally a better resistance to fretting wear when compared to junctions with proximal angular mismatches. Hence, in this paper, a small yet realistic distal angular mismatch (0.01°) was chosen for all the cases in order to investigate the influence of the assembly load.

The adaptive FE simulation was used to simulate the fretting wear process for one million loading cycles. An adaptive time stepping [28] was used in the simulations with an assumption of constant wear rate during a certain number of cycles (ΔN). After several preliminary simulations, it was found that ΔN should not be assumed the same for all the periods of loading cycles. Due to the existence of a very small mismatch angle in the geometry of the interface (distal contact type with an angular mismatch of 0.01°), large contact pressures were induced over the small contacting area at the first loading cycles, which showed that care should be taken for the selection of ΔN. During the fretting wear process, the contacting area expanded gradually, which then reduced the contact pressure. Therefore, ΔN was carefully changed from 50 to 800 loading cycles over the entire fretting wear process. The size of the elements was refined several times and 0.10 mm was found as the most suitable length of the element edge in the contact area, which could provide mesh-independent results. Figure 3a shows that the first layers of the head and neck materials at the interface were meshed with very small structured quadratic elements. These elements need to be small enough to correctly model the contact pressure and relative displacement over the contact area. The sublayers were then meshed by free-quad elements, which allow increased element sizes away from the contact area. The third part of the head and neck models was again meshed by relatively large structured elements. This meshing structure considerably reduced the solution time while providing accurate results. To simulate the interaction between the head and neck, both normal and tangential contact behaviors were defined. Normal contact was simulated using a surface-to-surface contact algorithm within ABAQUS via the "hard" contact option. The tangential interaction was modelled with a classical isotropic Coulomb friction model that was implemented with a stiffness (penalty) method.

The 2D fretting wear model of the CoCr/CoCr taper junction was assembled with four different assembly forces of 2000 N, 3000 N, 4000 N, and 5000 N. A PYTHON code and a MATLAB code were developed to report the contact pressures and relative micro-motions at the contact interface, and to find the material loss in the form of worn area from the surface at various cycles (up to 1,025,000 cycles) of normal walking gait loading.

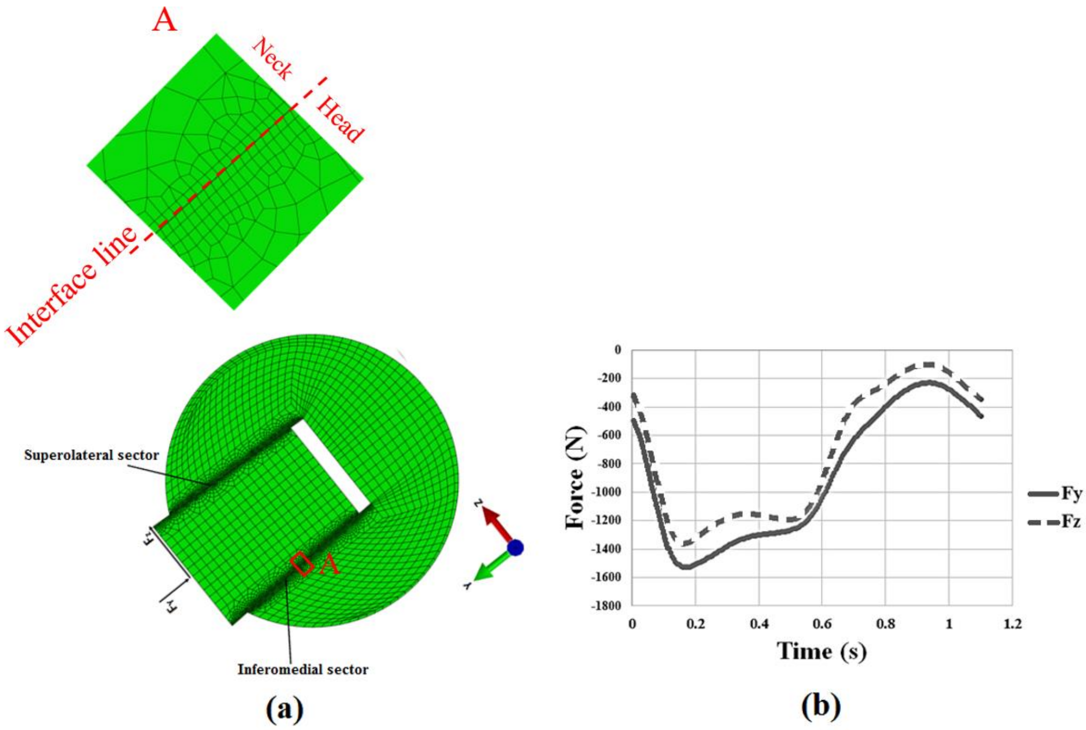

Figure 3. (**a**) Mesh structure of the 2D model of the most critical plane of the head-neck junction and (**b**) profile of corresponding forces in Y and Z axes from the normal walking gait cycle.

3. Results

3.1. Contact Pressure and Contact Length

As shown in Figure 4, when increasing the assembly force from 2000 N to 5000 N, the contact pressure increased in magnitude over the length of the neck, and the contacting region between the head and neck (contact length) also increased toward the proximal side of the neck. This confirms that a higher assembly force can further push the neck into the head, which induces greater normal contact forces. Thereby, larger contact pressures and more engagement between the head and neck surfaces (longer contact). As more loading cycles were applied (increase in the number of cycles), the peak contact pressure decreased in magnitude. The maximum magnitude of contact pressure for cases with assembly forces of 2000 N, 3000 N, 4000 N, and 5000 N decreased from 206, 257, 265, and 337 MPa at 25,000 cycles to 169, 243, 258, and 294 MPa at 1,025,000 cycles, respectively, in the super-lateral sector of the neck. These graphs can also help investigate the contact length between the head and neck. Non-zero contact stresses at any region of the surface indicate that there is contact between the head and neck in that region. After 25,000 cycles, the percentage of the neck, which is in contact with the head for cases with assembly forces of 2000 N, 3000 N, 4000 N, and 5000 N, were 48%, 64%, 75%, and 79%, respectively. These total contact lengths remained nearly constant after 1,000,000 cycles of fretting wear.

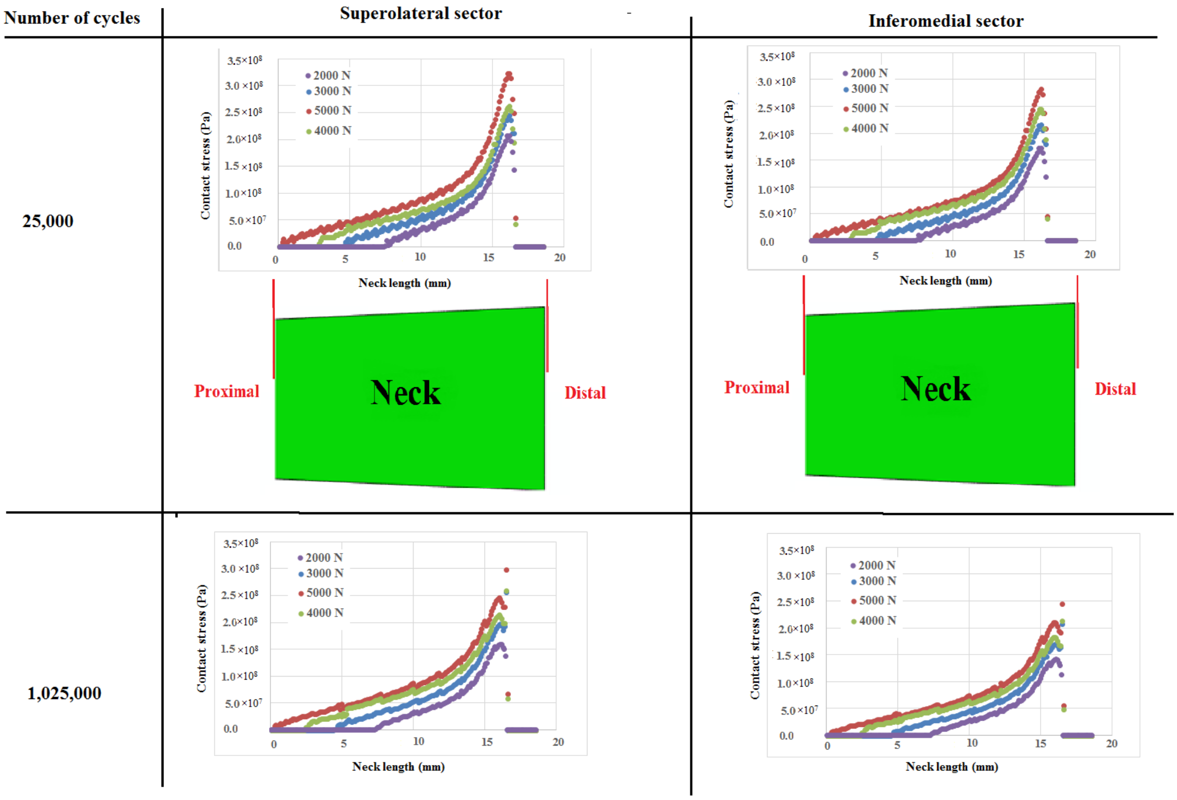

Figure 4. Variation of normal contact stress over the neck length in both super-lateral and infero-medial sectors under different assembly forces and after 25,000 and 1,025,000 loading cycles.

3.2. Micro-Motions

For all the assembly forces, the micro-motion at the contacting interface tends to increase from the proximal side to the distal side (Figure 5) and the magnitude of the micro-motion reduces when increasing the assembly force. The junction assembled with 2000 N had the largest micro-motions compared to the other cases with a range of 0.41 to 0.51 µm. There appears to be minimal changes in the micro-motion after 1,000,000 load cycles (Figure 5).

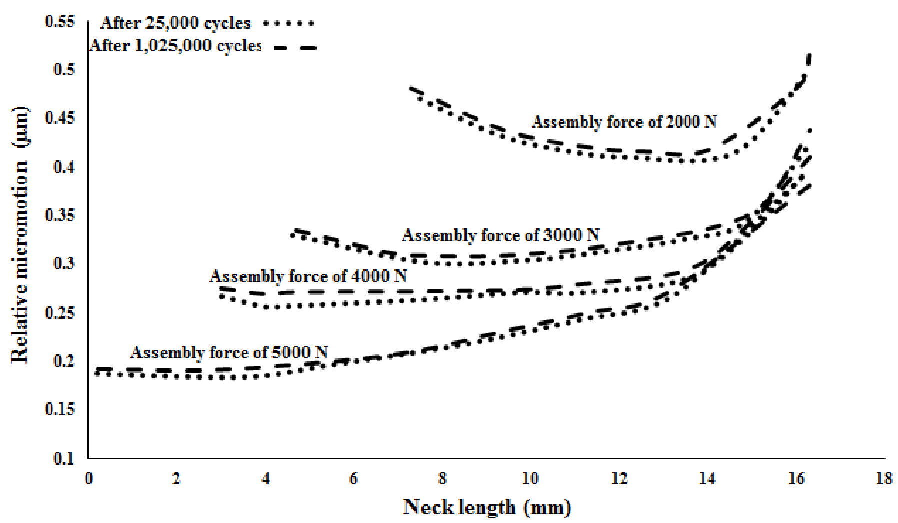

Figure 5. Relative micro-motion at the contacting interface over the neck length (super-lateral sector) for different assembly forces after 25,000 and 1,025,000 cycles.

3.3. Material Loss

Material removal over the neck length was calculated as the total area under the curve of wear depth versus the neck length in both the super-lateral and infero-medial sectors. This represents the lost area from the original edges (super-lateral and infero-medial sectors) of the 2D model. It can be seen in Figure 6a that the trend of the lost area over the number of loading cycles is linear for all of the assembly forces studied. The values of area loss for different assembly forces and at different cycles were almost equal in both the head and neck. Therefore, this figure only presents the area losses of the neck. Increasing the assembly force results in an increase in the lost area at the taper junction. For instance, when the assembly force was increased from 2000 N to 5000 N, the area loss increased from 5.28×10^{-3} mm^2 to 16.3×10^{-3} mm^2 in the neck after 1,025,000 cycles.

Figure 6b shows the effect of assembly force on the rate and location of the fretting wear damage in the form of wear depth (after 25,000 and 1,025,000 number of cycles) in the neck. It is noted that very similar depth of wear results were found in the head at the same number of cycles. These graphs can help compare the wear depth at different assembly forces, and locate the wear damage at the interface. It can be seen that the wear depths in the assembly force of 5000 N (with a maximum 0.779 μm) was significantly higher than that of the assembly force of 2000 N (with a maximum 0.413 μm).

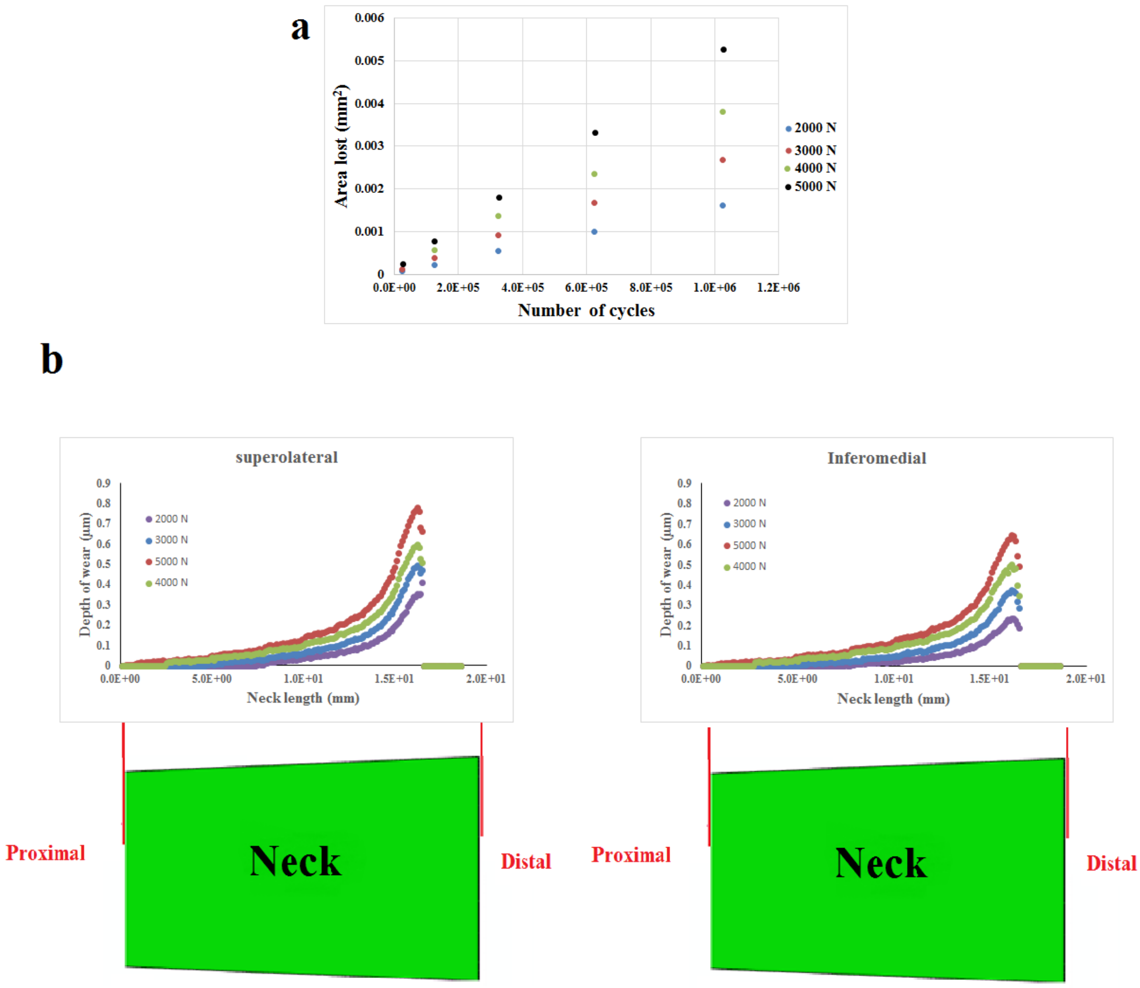

Figure 6. (**a**) Lost area versus number of cycles for different assembly forces and (**b**) depth of wear over the neck length after 1,025,000 cycles.

4. Discussion

In this work, the fretting wear mechanism and material loss were investigated in a CoCr/CoCr head-neck junction with a real angular mismatch in a PBS solution and under normal walking gait loading. The junction was assembled with various forces ranging from 2 kN to 5 kN to represent low-to-high impaction forces applied by surgeons in practice. The area loss from the edges of the most critical plane of the junction (as an indicator of material loss in the junction) showed a linearly increasing pattern over the fretting wear cycles. This could help estimate the degree of material loss after several million cycles of fretting wear.

The results of this work revealed that contact pressure, contact length, and relative micro-motion at the interface of the junction are the key parameters that can influence the material loss caused by fretting wear. Figure 5 showed that, when increasing the assembly force, relative micro-motion between the head and neck components reduces considerably, which offers more stability to the junction. According to the Archard equation, wear is proportional to both the contact pressure and relative micro-motion (amplitude of sliding). Even though the relative micro-motions decrease in the firmly assembled junctions, the significant increase in the contact pressure (induced over greater contact regions) leads to a net increase in fretting wear and, consequently, material removal. The results showed that a higher assembly force can induce a longer contact at the interface. This can extend the surface on which fretting wear is to occur and can, therefore, increase the extent of material removal. As shown in Figure 6a (for the studied taper design and material combination), increasing the assembly force results in more material loss. This is in contrast with the English's results [22] where higher assembly forces were reported to reduce fretting wear. On the other hand, Bitter's experimental results [18] showed no rational relation between the assembly force and the volumetric wear. The wear volume reduced when increasing the assembly force from 2 kN to 4 kN, and then slightly increased when increasing the assembly force from 4 kN to 15 kN. They found large standard deviations in their wear volume results (no significant difference between the three tested assembly forces). Bitter's FE simulations were too simplified and did not incorporate geometry updates to account for material loss due to the process of fretting wear. One immediate difference between the two previously mentioned studies and the present work is the material combination. In this study, the material combination is CoCr/CoCr, while they used CoCr/Ti and Ti/Ti combinations. Material properties, particularly the modulus of elasticity, can influence the behavior of the contact, especially the relative micro-motion. The angular mismatch within the junction is the major difference between the present work and their studies. The authors have previously shown that the existence of angular mismatch has a significant effect on the contact length, contact pressure, relative micro-motion, and, accordingly, the wear damage [23]. In English's model, zero mismatch was assumed between the head and neck taper angles. Therefore, the contact length would always be constant (due to having no angular mismatch).Furthermore, increasing the assembly force reduces the relative micro-motion at the head-neck interface, which, in turn, reduces the amount of material loss. However, in this work, the contact between the head and neck is not perfect. Therefore, increasing the assembly force increases the contact length in the head-neck junction, which results in increasing the material loss. Bitter's et al. [18] did not mention if there was an actual angular mismatch in their head-neck samples. Therefore, valid statements cannot be made to directly compare and discuss their results with those of this study in terms of the mismatch angle's influence.

Assembly force, as an intraoperative surgical parameter, can play an important role in the fretting wear damage to the head and neck components. This study was developed for a particular design including a CoCr/CoCr material combination with a distal angular mismatch of 0.01°. This, together with the contradicting results reported previously [18,23], may suggest that further research is required to investigate the influence of the assembly force on the fretting wear behavior, considering various angular mismatches as well as different material combinations and loading profiles of other daily activities before making a certain suggestion to clinicians in terms of a recommended force for assembling head-neck taper junctions. Moreover, fretting corrosion in the head-neck taper junction is a combination of mechanical fretting wear and electro-chemical corrosion processes. The scope of this study was to investigate the influence of assembly force (as a mechanical parameter) on the material loss at the head-neck junction of hip implants. Hence, the model was developed to simulate only the mechanical fretting wear process in the junction. However, corrosion can play an important role in the behavior of the contact and, thus, the amount of material loss. The authors of this study have developed a new adaptive finite element model to simulate fretting corrosion at metallic interfaces [30]. This model has been successfully used to simulate fretting corrosion for only a simple geometry. Further research is required to use this new and complex model to simulate fretting wear corrosion in head-neck taper junctions.

5. Conclusions

High assembly forces reduce the relative micro-motions between the head and neck at the taper junction. However, they can also increase the contact pressures and the contact region at the interface, which, in turn, may intensify the fretting wear process and, consequently, increased material removal. The results of this study showed that the effect of the last two parameters (contact pressure and contact length) was more dominant in wearing out the surface of the studied CoCr/CoCr junction with a taper angle mismatch of 0.01°. Hence, when increasing the assembly force, the degree of material loss increased for this particular design and material combination of the junction studied in this work.

Author Contributions: Conceptualization, K.F., R.H.O. and M.T.; Data curation, K.F. and H.B.; Formal analysis, K.F., R.H.O. and M.T.; Methodology, K.F., R.H.O., H.B. and M.T.; Resources, R.H.O.; Software, M.T.; Supervision, R.H.O. and M.T.; Validation, K.F. and R.H.O.; Visualization, K.F.; Writing—original draft, K.F. and R.H.O.; Writing—review & editing, R.H.O. and M.T.

Funding: This research received no external funding.

Acknowledgments: The authors acknowledge the support of an Australian Government Research Training Program Scholarship for Khosro Fallahnezhad's PhD.

Conflicts of Interest: The authors have no conflict of interest to declare.

References

1. Gilbert, J.L.; Buckley, C.A.; Jacobs, J.J. In vivo corrosion of modular hip prosthesis components in mixed and similar metal combinations. The effect of crevice, stress, motion, and alloy coupling. *J. Biomed. Mater. Res.* **1993**, *27*, 1533–1544. [CrossRef] [PubMed]
2. Oskouei, R.; Fallahnezhad, K.; Kuppusami, S. An Investigation on the Wear Resistance and Fatigue Behaviour of Ti-6Al-4V Notched Members Coated with Hydroxyapatite Coatings. *Materials* **2016**, *9*, 111. [CrossRef] [PubMed]
3. Chana, R.; Esposito, C.; Campbell, P.A.; Walter, W.K.; Walter, W.L. Mixing and matching causing taper wear: Corrosion associated with pseudotumour formation. *J. Bone Joint Surg. Br.* **2012**, *94*, 281–286. [CrossRef]
4. Fricka, K.B.; Ho, H.; Peace, W.J.; Engh, C.A., Jr. Metal-on-Metal Local Tissue Reaction Is Associated With Corrosion of the Head Taper Junction. *J. Arthroplast.* **2012**, *27*, 26–31. [CrossRef]
5. Hussenbocus, S.; Kosuge, D.; Solomon, L.B.; Howie, D.W.; Oskouei, R.H. Head-neck taper corrosion in hip arthroplasty. *BioMed Res. Int.* **2015**, *2015*, 9. [CrossRef]
6. Fallahnezhad, K.; Farhoudi, H.; Oskouei, R.H.; Taylor, M. Influence of geometry and materials on the axial and torsional strength of the head-neck taper junction in modular hip replacements: A finite element study. *J. Mech. Behav. Biomed. Mater.* **2016**, *60*, 118–126. [CrossRef] [PubMed]
7. Donaldson, F.E.; Coburn, J.C.; Siegel, K.L. Total hip arthroplasty head-neck contact mechanics: A stochastic investigation of key parameters. *J. Biomech.* **2014**, *47*, 1634–1641. [CrossRef]
8. Gührs, J.; Körner, M.; Bechstedt, M.; Krull, A.; Morlock, M.M. Stem taper mismatch has a critical effect on ceramic head fracture risk in modular hip arthroplasty. *Clin. Biomech.* **2017**, *41*, 106–110. [CrossRef] [PubMed]

9. Kocagöz, S.B.; Underwood, R.J.; Sivan, S.; Gilbert, J.L.; MacDonald, D.W.; Day, J.S.; Kurtz, S.M. Does Taper Angle Clearance Influence Fretting and Corrosion Damage at the Head-Stem Interface? A Matched Cohort Retrieval Study. *Semin. Arthroplast.* **2013**, *24*, 246–254. [CrossRef]
10. Farhoudi, H.; Fallahnezhad, K.; Oskouei, R.H.; Taylor, M. A finite element study on the mechanical response of the head-neck interface of hip implants under realistic forces and moments of daily activities: Part 1, level walking. *J. Mech. Behav. Biomed. Mater.* **2017**, *75*, 470–476. [CrossRef]
11. Fallahnezhad, K.; Farhoudi, H.; Oskouei, R.H.; Taylor, M. A finite element study on the mechanical response of the head-neck interface of hip implants under realistic forces and moments of daily activities: Part 2. *J. Mech. Behav. Biomed. Mater.* **2018**, *77*, 164–170. [CrossRef]
12. Rehmer, A.; Bishop, N.E.; Morlock, M.M. Influence of assembly procedure and material combination on the strength of the taper connection at the head-neck junction of modular hip endoprostheses. *Clin. Biomech. (Bristol, Avon)* **2012**, *27*, 77–83. [CrossRef] [PubMed]
13. Georgiou, G.; Siapkara, A.; Dimitrakopoulou, A.; Provelengios, S.; Dounis, E. Dissociation of bipolar hemiarthroplasty of the hip after dislocation. *Injury* **2006**, *37*, 162–168. [CrossRef]
14. Ramoutar, D.N.; Crosnier, E.A.; Shivji, F.; Miles, A.W.; Gill, H.S. Assessment of Head Displacement and Disassembly Force With Increasing Assembly Load at the Head/Trunnion Junction of a Total Hip Arthroplasty Prosthesis. *J. Arthroplast.* **2017**, *32*, 1675–1678. [CrossRef] [PubMed]
15. Nassutt, R.; Mollenhauer, I.; Klingbeil, K.; Henning, O.; Grundei, H. Relevance of the insertion force for the taper lock reliability of a hip stem and a ceramic femoral head. *Biomed. Tech. Biomed. Eng.* **2006**, *51*, 103–109. [CrossRef] [PubMed]
16. Pennock, A.T.; Schmidt, A.H.; Bourgeault, C.A. Morse-type tapers: Factors that may influence taper strength during total hip arthroplasty. *J. Arthroplast.* **2002**, *17*, 773–778. [CrossRef]
17. Scholl, L.; Longaray, J.; Raja, L.; Lee, R.; Faizan, A.; Herrera, L.; Thakore, M.; Nevelos, J. Friction in modern total hip arthroplasty bearings: Effect of material, design, and test methodology. *Proc. Inst. Mech. Eng. Part H J. Eng. Med.* **2015**, *230*, 50–57. [CrossRef]
18. Bitter, T.; Khan, I.; Marriott, T.; Lovelady, E.; Verdonschot, N.; Janssen, D. A combined experimental and finite element approach to analyse the fretting mechanism of the head-stem taper junction in total hip replacement. *Proc. Inst. Mech. Eng. Part H J. Eng. Med.* **2017**, *231*, 862–870. [CrossRef] [PubMed]
19. Witt, F.; Gührs, J.; Morlock, M.M.; Bishop, N.E. Quantification of the contact area at the head-stem taper interface of modular hip prostheses. *PLoS ONE* **2015**, *10*, e0135517. [CrossRef]
20. Dyrkacz, R.M.R.; Brandt, J.M.; Morrison, J.B.; O'Brien, S.T.; Ojo, O.A.; Turgeon, T.R.; Wyss, U.P. Finite element analysis of the head-neck taper interface of modular hip prostheses. *Tribol. Int.* **2015**, *91*, 206–213. [CrossRef]
21. English, R.; Ashkanfar, A.; Rothwell, G. A computational approach to fretting wear prediction at the head–stem taper junction of total hip replacements. *Wear* **2015**, *338–339*, 210–220. [CrossRef]
22. English, R.; Ashkanfar, A.; Rothwell, G. The effect of different assembly loads on taper junction fretting wear in total hip replacements. *Tribol. Int.* **2016**, *95*, 199–210. [CrossRef]
23. Fallahnezhad, K.; Oskouei, R.H.; Badnava, H.; Taylor, M. An adaptive finite element simulation of fretting wear damage at the head-neck taper junction of total hip replacement: The role of taper angle mismatch. *J. Mech. Behav. Biomed. Mater.* **2017**, *75*, 58–67. [CrossRef] [PubMed]
24. Farhoudi, H.; Oskouei, R.H.; Jones, C.F.; Taylor, M. A novel analytical approach for determining the frictional moments and torques acting on modular femoral components in total hip replacements. *J. Biomech.* **2015**, *48*, 976–983. [CrossRef] [PubMed]
25. Farhoudi, H.; Oskouei, R.; Pasha Zanoosi, A.; Jones, C.; Taylor, M. An Analytical Calculation of Frictional and Bending Moments at the Head-Neck Interface of Hip Joint Implants during Different Physiological Activities. *Materials* **2016**, *9*, 982. [CrossRef]
26. Archard, J. Contact and rubbing of flat surfaces. *J. Appl. Phys.* **1953**, *24*, 981–988. [CrossRef]
27. Johansson, L. Numerical Simulation of Contact Pressure Evolution in Fretting. *J. Tribol.* **1994**, *116*, 247–254. [CrossRef]
28. Ding, J.; Leen, S.B.; McColl, I.R. The effect of slip regime on fretting wear-induced stress evolution. *Int. J. Fatigue* **2004**, *26*, 521–531. [CrossRef]
29. McColl, I.R.; Ding, J.; Leen, S.B. Finite element simulation and experimental validation of fretting wear. *Wear* **2004**, *256*, 1114–1127. [CrossRef]

30. Fallahnezhad, K.; Oskouei, R.H.; Taylor, M. Development of a fretting corrosion model for metallic interfaces using adaptive finite element analysis. *Finite Elem. Anal. Des.* **2018**, *148*, 38–47. [CrossRef]
31. Maruyama, N.; Kawasaki, H.; Yamamoto, A.; Hiromoto, S.; Imai, H.; Hanawa, T. Friction-wear properties of nickel-free co-cr-mo alloy in a simulated body fluid. *Mater. Trans.* **2005**, *46*, 1588–1592. [CrossRef]